Journal of Advanced Ceramics

Volume 7 | Issue 1 Article 1

2018

Bi/Bi_2O_3 sensor for quantitation of dissolved oxygen in molten salts

Huiping ZHENG
East China Normal University, Shanghai 200241, China

Hongqiang NIAN
Shanghai Institute of Ceramics, Chinese Academy of Sciences, Shanghai 201899, China

Jinfeng XIA
Shanghai Institute of Ceramics, Chinese Academy of Sciences, Shanghai 201899, China

Guohong ZHOU
Shanghai Institute of Ceramics, Chinese Academy of Sciences, Shanghai 201899, China

Danyu JIANG
Shanghai Institute of Ceramics, Chinese Academy of Sciences, Shanghai 201899, China

See next page for additional authors

Recommended Citation
Huiping ZHENG, Hongqiang NIAN, Jinfeng XIA et al. Bi/Bi2O3 sensor for quantitation of dissolved oxygen in molten salts. Journal of Advanced Ceramics 2018, 07(01): 1-4.

Journal of Advanced Ceramics
2018, **7**(1): 1–4
https://doi.org/10.1007/s40145-017-0250-4
ISSN 2226-4108
CN 10-1154/TQ

Research Article

Bi/Bi_2O_3 sensor for quantitation of dissolved oxygen in molten salts

Huiping ZHENG[a], Hongqiang NIAN[b], Jinfeng XIA[b], Guohong ZHOU[b], Danyu JIANG[b], Qiang LI[a,*]

[a]*East China Normal University*, *Shanghai 200241*, *China*
[b]*Shanghai Institute of Ceramics*, *Chinese Academy of Sciences*, *Shanghai 201899*, *China*

Received: August 16, 2017; Accepted: October 02, 2017

Abstract: To quantify the oxygen content in molten salts, we examined the performance of an yttria-stabilized zirconia solid electrolyte oxygen sensor with a Bi/Bi_2O_3 reference electrode, focusing on its output accuracy. When the above sensor was tested in a flow of gas with known oxygen partial pressure, p_{O_2}, a linear relationship between $\lg p_{O_2}$ and the electromotive force (EMF) was observed, and the correlation slope exhibited a positive deviation from Nernstian behavior. EMF measurements performed in molten NaCl–KCl indicated that the oxygen content of this salt mixture increased with increasing oxygen partial pressure in the covering gas, in agreement with Henry's law. Moreover, the EMF exhibited a linear decrease with increasing melt temperature of molten NaCl–KCl, in agreement with the theoretical model. Finally, a relationship between the structure of molten NaCl–KCl and its oxygen diffusion behavior was established. As a result, the developed sensor was demonstrated to be well suited for determining the oxygen content of molten salts.

Keywords: molten salt; oxygen sensor; Bi/Bi_2O_3; oxygen content

1 Introduction

Molten salts remain liquid in a wide temperature range, exhibiting stability at high temperatures, low vapor pressure, ability to dissolve numerous inorganic and organic compounds, low viscosity (due to ions being mutually independent), and high heat capacity per unit volume [1,2], being broadly utilized as engineering fluids with a wide range of applications, e.g., catalytic medium for coal gasification, waste oxidation, sensible heat storage, and molten salt reactors [3–6]. The development of the above mentioned technologies increases the requirements placed on the composition and properties of molten salts, such as the content of dissolved oxygen. Although the latter parameter significantly affects molten salt processing [7], posing a number of safety threats to operating molten salt reactors (such as reducing the solubility of nuclear fuel and promoting the slow precipitation of uranium oxide), no corresponding uniform and universal quantitation methods exist [8–10].

The molten salt technology can be traced back the dawn of the nineteenth century, when Humphrey Davy employed it to isolate alkali metals [11–13]. Currently, molten salts are increasingly used in the energy industry, mainly in the fields of solar and thermal energy storage [14–16]. Volkovic *et al.* [17] developed a novel sensitive method for determining oxygen solubility in molten carbonates and carbonate-based melts, revealing that measurements at various partial pressures of oxygen allowed the determination of

* Corresponding author.
E-mail: qli@chem.ecnu.edu.cn

predominant oxygen species in the melt and examining the applicability of Henry's law to this system. Phongikaroon *et al.* [18] used a high-speed digital camera to analyze oxygen bubble distributions in LiCl–KCl melts at 723 K produced at different sparging rates.

In this work, the oxygen content of molten salts exposed to covering gases with different oxygen partial pressures and its temperature dependence were measured using a Bi/Bi_2O_3 sensor.

2 Experimental

The Bi/Bi_2O_3 oxygen sensor comprised a solid electrolyte, a reference electrode, an electrode wire, and an auxiliary electrode (Fig. 1). A cylinder of 8 mol% yttria-stabilized zirconia (YSZ) formed by sintering commercially available YSZ powder was used as the solid electrolyte. The reference electrode contained a mixture of bismuth (99.9%, Aladdin, China) and bismuth oxide (analytical reagent, Aladdin, China) in a mole ratio of 95:5, and the electrode wire was composed of Mo. The sensor was sealed using a high-temperature glass-binding agent.

All experiments were performed under static conditions in a tube furnace (JCL11, China) at 973–1073 K.

The setup used to determine the oxygen content of molten NaCl–KCl is shown in Fig. 1. Commercially available NaCl and KCl (analytical reagent, Guoyao, China) were placed in an Al_2O_3 crucible and heated in the tube furnace. The EMF of the Bi/Bi_2O_3 sensor in the molten salt mixture was measured at 973 K for covering gases with different oxygen contents (i.e., high-purity N_2 (99.999%, 200 vppm O_2) and N_2+O_2 (0.5, 1.0, and 2.5 vol%)) and at different temperatures (973–1073 K) in a covering gas of high-purity N_2/200 vppm O_2. The gas concentration and flow rate were controlled using a mass flow meter, and EMF values were recorded using a voltmeter (34972A, Agilent).

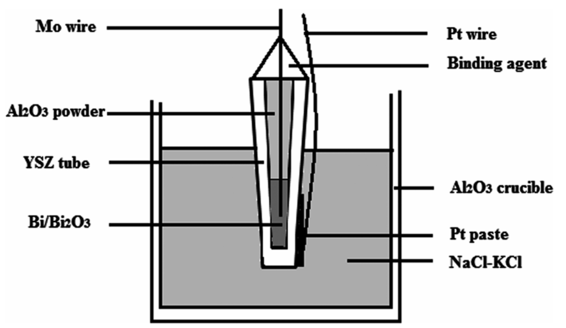

Fig. 1 Setup used to determine the oxygen content of molten NaCl–KCl.

3 Results and discussion

The utilization of oxygen sensors for characterizing molten salts is expected to achieve better accuracy, outperforming gas-phase measurements due to requiring less experimental effort and time for adjusting a predictable oxygen potential.

Figure 2 shows the results of accuracy measurements obtained for the abovementioned sensor, revealing that at constant temperature, the logarithm of gas-phase oxygen activity was linearly correlated with the EMF, which decreased with increasing temperature.

The following oxidation and reduction processes are involved in sensor operation:

$$4Bi + 6O^{2-} \rightarrow 2Bi_2O_3 + 12e^- \quad (1)$$

$$3O_2 + 12e^- \rightarrow 6O^{2-} \quad (2)$$

with the overall cell reaction represented as

$$4Bi + 3O_2 \rightarrow 2Bi_2O_3 \quad (3)$$

Thus,

$$E = (-2\,\Delta_f G^0(Bi_2O_3) + 3RT\ln p_{O_2})/12F \quad (4)$$

The Gibbs free energy of oxide formation can be expressed as

$$\Delta_f G^0(Bi_2O_3) = -386790 + 188.95T \quad (5)$$

affording

$$E = 0.668 - 3.26 \times 10^{-4}T + 4.96 \times 10^{-5}T\lg p_{O_2} \quad (6)$$

where E is the EMF value (V), T is the temperature (K). Therefore, the relationship between $\lg p_{O_2}$ and the EMF should be linear at constant temperature. The slope of the EMF vs. $\lg p_{O_2}$ plot is an important sensor characteristic, with experimental values exceeding

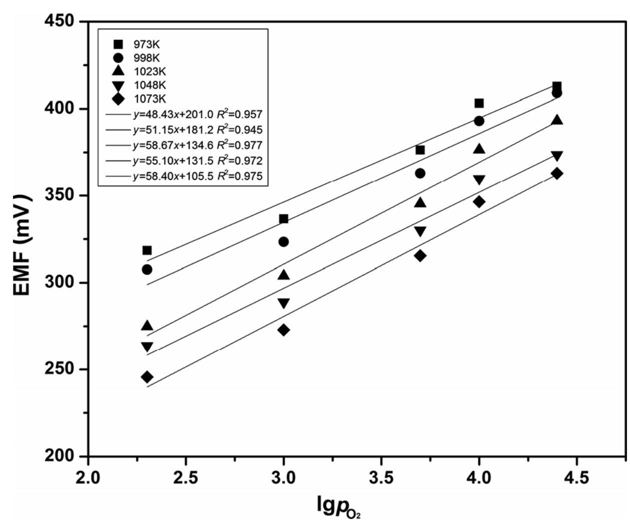

Fig. 2 Results of accuracy measurements performed using the Bi/Bi_2O_3 sensor at variable temperatures.

theoretical ones, as shown in Fig. 3. This deviation increased at elevated temperatures, possibly due to the additional reaction of O^{2-} with YSZ in the Bi/Bi_2O_3 reference electrode:

$$O^{2-} \rightarrow O + 2e^- \tag{7}$$

Since atomic O exhibits a certain solubility in molten metals at low temperatures, this reaction can influence the EMF and cause the observed deviation.

The output-corrected Bi/Bi_2O_3 sensor was used to determine the oxygen content of molten NaCl–KCl.

Initially, the effects of covering gases with different oxygen partial pressures on the output signal were investigated at 973 K. Based on the plots shown in Fig. 2, the oxygen content ($a_{O\ salt}$) of molten NaCl–KCl was calculated for covering gases with different p_{O_2}, with the results shown in Fig. 4. The above figure reveals that the EMF increased with increasing p_{O_2}, indicating that the oxygen content of molten NaCl–KCl was significantly lower than the saturation value, increasing with the concentration of oxygen in the covering gas.

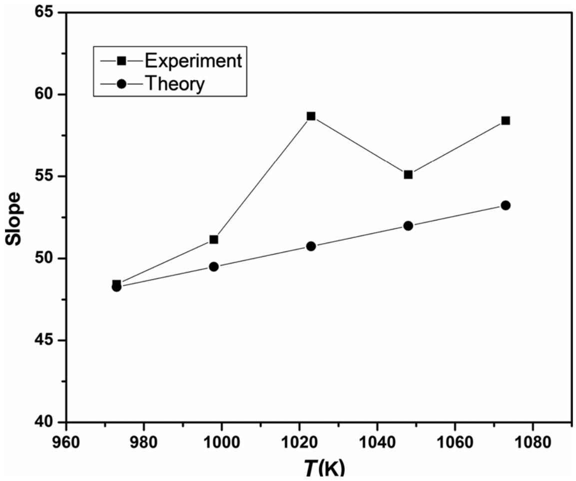

Fig. 3 Deviation between measured and theoretical slopes of EMF vs. $\lg p_{O_2}$ plots as a function of temperature.

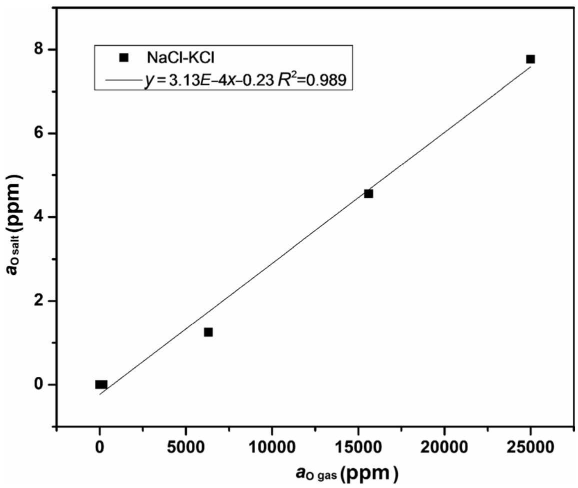

Fig. 4 Oxygen content ($a_{O\ salt}$) of molten NaCl–KCl as a function of O_2 partial pressure ($a_{O\ gas}$) in covering gases.

The solubility of O_2 in molten salts is commonly described by Henry's law, implying a linear relationship between oxygen solubility and its partial pressure in the covering gas. In fact, the structure of molten salts is similar to that of liquids, justifying the use of the above model, which well fitted experimental data (Fig. 4). Based on the experimental results, the following relationship was established:

$$a_{O\ salt} = 3.14 \times 10^{-4}\ a_{O\ gas} - 0.23 \tag{8}$$

Thus, Henry's law is well suited for explaining the behavior of oxygen in molten NaCl–KCl, which can be thought to exhibit short-range order and contain a large number of defects, allowing the diffusion of oxygen molecules. Thus, the behavior of oxygen in molten NaCl–KCl is similar to that in a liquid, allowing a large amount of oxygen to be adsorbed and thus resulting in a high EMF.

Since temperature plays an important role in determining the accuracy and range of oxygen concentration measurements, its effect on the above parameters was also explored.

The temperature dependences of EMF in molten NaCl–KCl for covering gases containing 200 vppm and 0.5 vol% O_2 are shown in Fig. 5, exhibiting linearity under both conditions and high fitting precision. Thus, the above dependence at 200 vppm O_2 was expressed as

$$E = -0.0046T + 5.22 \tag{9}$$

and that at 0.5 vol% O_2 was given by

$$E = -0.0056T + 5.93 \tag{10}$$

Moreover, the EMF decreased with increasing temperature, in agreement with Eq. (6).

4 Conclusions

The performance of a Bi/Bi_2O_3 oxygen sensor was systematically examined at different temperatures in flows of gases with different O_2 partial pressures, revealing an obvious deviation from Nernstian behavior. The sensor output was corrected and used to determine the oxygen content of molten NaCl–KCl, which increased with increasing O_2 partial pressure, in agreement with Henry's law. In accordance with the theoretical model, the EMF exhibited a linear decrease with increasing

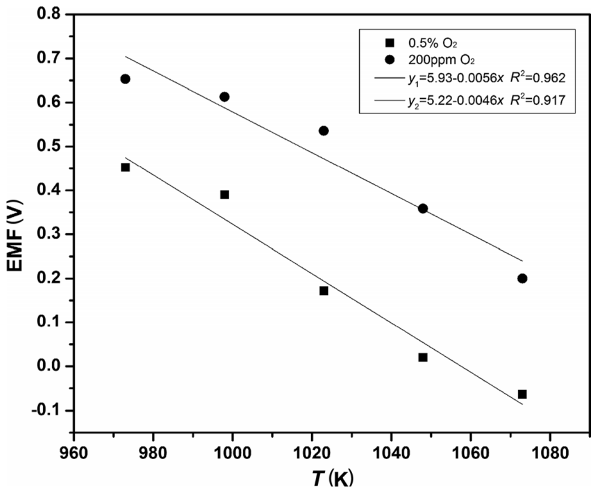

Fig. 5 Dependence of EMF on temperature in molten NaCl–KCl.

temperature of molten NaCl–KCl. Overall, the prepared sensor showed reliable behavior, thus being suitable for determining the concentration of dissolved oxygen in molten salts, which is an integral part of numerous industrial processes.

Acknowledgements

The author thanks the Shanghai Institute of Ceramics and Chinese Academy of Sciences for support.

References

[1] Serrano-López R, Fradera J, Cuesta-López S. Molten salts database for energy applications. *Chem Eng Process* 2013, **73**: 87–102.

[2] Liu Q, Bai Z, Sun J, *et al*. Thermodynamics investigation of a solar power system integrated oil and molten salt as heat transfer fluids. *Appl Therm Eng* 2016, **93**: 967–977.

[3] Wang W, Li H, Guo Y, *et al*. Mullite whiskers prepared by molten salt method using Si powders. *J Adv Ceram* 2012, **1**: 283–289.

[4] Herrmann U, Kelly B, Price H. Two-tank molten salt storage for parabolic trough solar power plants. *Energy* 2004, **29**: 883–893.

[5] García López J, Respaldiza MA, Siejka J, *et al*. Use of nuclear microanalysis to study the oxygenation mechanism of $Y_1Ba_2Cu_3O_{7-x}$ thin films: Estimation of the oxygen diffusion coefficients. *Nucl Instrum Meth B* 2002, **190**: 661–666.

[6] Cho Y-Z, Yang H-C, Park G-H, *et al*. Treatment of a waste salt delivered from an electrorefining process by an oxidative precipitation of the rare earth elements. *J Nucl Mater* 2009, **384**: 256–261.

[7] Nunes VMB, Lourenco MJV, Santos FJV, *et al*. Importance of the accurate data on viscosity and thermal conductivity in molten salts applications. *J Chem Eng Data* 2003, **48**: 446–450.

[8] Frangini S, Scaccia S. The role of foreign cations in enhancing the oxygen solubility properties of alkali molten carbonate systems: Brief survey of existing data and new research results. *Int J Hydrogen Energ* 2014, **39**: 12266–12272.

[9] Imanaka N, Masui T, Jyoko K. Selective liquid phase oxidation of cyclohexane over $Pt/CeO_2–ZrO_2–SnO_2/SiO_2$ catalysts with molecular oxygen. *J Adv Ceram* 2015, **4**: 111–117.

[10] Gao X, Liu T, Yu J, *et al*. Limiting current oxygen sensor based on $La_{0.8}Sr_{0.2}Ga_{0.8}Mg_{0.2}O_{3-\delta}$ as both dense diffusion barrier and solid electrolyte. *Ceram Int* 2017, **43**: 6329–6332.

[11] Lovering DG. *Molten Salt Technology*. NY: Plenum Press, 1982.

[12] Papatheodorou GN. Molten salts for two centuries. *Molten Salts Bull* 2005, **83**: 1–6.

[13] Gaune-Escard M. *Molten Salts: From Fundamentals to Applications*. Dordrecht: Kluwer Acad. Publ., 2002.

[14] Volkovich VA, Griffiths TR, Fray DJ, *et al*. Oxidation of ceramic uranium dioxide in alkali metal carbonate-based melts: A study using various oxidants and comparison with UO_2 powder. *J Nucl Mater* 1998, **256**: 131–138.

[15] Kearney D, Kelly B, Herrmann U, *et al*. Engineering aspects of a molten salt heat transfer fluid in a trough solar field. *Energy* 2004, **29**: 861–870.

[16] Menéndez RP, Martínez JÁ, Prieto MJ, *et al*. A novel modeling of molten-salt heat storage systems in thermal solar power plants. *Energies* 2014, **7**: 6721–6740.

[17] Volkovic VA, Griffiths TR, Fray DJ, *et al*. A new method for determining oxygen solubility in molten carbonates and carbonate–chloride mixtures using the oxidation of UO_2 to uranate reaction. *J Nucl Mater* 2000, **282**: 152–158.

[18] Phongikaroon S, Bezzant RW, Simpson MF. Measurements and analysis of oxygen bubble distributions in LiCl–KCl molten salt. C*hem Eng Res Des* 2013, **91**: 418–425.